CELLULOSE NANOFIBERS OF OIL PALM BIOMASS IN ALGINATE-BASED MEMBRANES FOR WATER-ETHANOL MIXTURE SEPARATION

NOVITRI HASTUTI,[*,**] HENDRIK SETIAWAN,[***] KYOHEI KANOMATA[****] and TAKUYA KITAOKA[*****]

[*]*National Research and Innovation Agency, Research Center for Biomass and Bioproducts, Soekarno Science Center, Jl. Raya Jakarta-Bogor No. KM 46, Bogor, West Java, 16911, Indonesia*
[**]*Research Collaboration Center for Nanocellulose BRIN – Universitas Andalas, Padang, 25163, Indonesia*
[***]*Department of Hydrogen Energy Systems, Faculty of Engineering, Kyushu University, Motooka 744 Nishi-ku, Fukuoka, 819-0395, Japan*
[****]*Graduate School of Pharmaceutical Sciences, Osaka University, 1-6 Yamadaoka, Suita-shi, Osaka, 565-0871, Japan*
[*****]*Department of Agro-Environmental Sciences, Faculty of Agriculture, Kyushu University, Motooka 744 Nishi-ku, Fukuoka, 819-0395, Japan*
✉ *Corresponding author: N. Hastuti, novi043@brin.go.id, novitri.forester@gmail.com*

Received April 25, 2022

TEMPO-oxidized cellulose nanofibers (TOCNs) from waste of oil palm empty fruit bunches (OPEFB) were integrated into an alginate matrix to increase the capacity of the alginate membrane for water-ethanol separation. The membrane composed of the alginate matrix and TOCNs was characterized in terms of its morphological, physical-mechanical properties and performance in the separation of water-ethanol suspensions, with ethanol concentrations in the suspension of 10% and 20%. Other alginate membranes integrated with commercial TOCNs from wood were also prepared and tested for comparison. The results showed that the addition of TOCNs (made from wood and OPEFB waste) to the alginate matrix improved the water adsorption capacity of the membrane. The water adsorption capacity of the alginate membranes with wood-derived TOCNs, OPEFB-derived TOCNs and alginate only was 78%, 87% and 66%, respectively. The flux capacity of the alginate membrane, integrated with OPEFB-derived TOCNs, was higher than that of the alginate membrane alone, but lower than that of the alginate membrane integrated with wood-derived TOCNs. This study showed the utilization of nanocellulose from palm oil biomass waste can be considered to improve the physical-mechanical properties of alginate-based membranes used for various applications, including filtration.

Keywords: cellulose, membrane, nanofibers, oil palm, TOCNs

INTRODUCTION

Indonesia is the world's largest producer and exporter of palm oil in the world.[1] Therefore, oil palm (*Elaeis guineensis*) is the mainstay of estate crop commodity in Indonesia, its contribution to the national economy tends to increase from year to year and is expected to strengthen overall national development.[2] In addition, crude palm oil (CPO) production leaves an abundant supply of palm press fibres and oil palm empty fruit bunches (OPEFB), which are regarded as wastes and have not been utilized satisfactorily.[3] The palm oil industry must dispose of about 1.1 tons of OPEFB for every ton of CPO produced.[4]

It is essential that the huge amount of OPEFB is processed into value-added products as OPEFB contains a relatively high amount of cellulose, of about 59%.[5] Cellulose is an abundant natural polymer that can be extracted from plants, animals, algae, and bacteria.[6] Cellulosic fibers have gained consideration due to their promising characteristics, such as biodegradability, renewability, and high mechanical properties, as a result of their crystalline organization.[7] With its relatively high content of cellulose, OPEFB is a potential source of nanocellulose raw materials. In general, the term "nanocellulose" refers to a cellulosic extract or processed material that has nano-scale structural dimensions.[6] One of the useful methods that enable cellulose fibers to be completely converted to individual cellulose nanofibrils is catalytic oxidation using 2,2,6,6-tetramethylpiperidine 1-oxyl

(TEMPO). By using a TEMPO/NaBr/NaClO oxidation system, this process can convert selectively the primary hydroxyl groups of polysaccharides into carboxylates; fully individualized TEMPO-oxidized cellulose fibrils of approximately 4 nm in width and at least a few micrometers in length can be obtained, with carboxylate contents of more than about 1 mmol/g by mild mechanical disintegration in water.[8,9] Nanocellulose produced by 2,2,6,6-tetramethylpiperidine 1-oxyl (TEMPO)-catalyzed oxidation, named TEMPO-oxidized cellulose nanofibers (TOCNs), has attracted considerable attention, since it requires low energy in its production, making the narrowest nanofibers ever reported.[10] Furthermore, the results of our previous study showed that nanocellulose from oil palm empty fruit bunches produced through hydrolysis of hydrochloric acid had an aspect ratio ranging between 23-29, and thermal stability between 347-359 ºC as maximum degradation temperature.[11]

Recently, TOCNs have seen several applications, including for green reinforcement in polymer composites, as an adsorbent for metal removal, and as a gel component for medical applications (drug delivery).[12-15] Furthermore, nanocellulose in polymer composites can be applied as a filler or hydrophilic additive in membranes by blending or coating technique and in ultrafiltration and separation membrane for gas capturing and bioenergy recovery.[16,17] The use of nanocellulose in membrane composites also increases biofouling resistance in membranes by forming a thin layer on top of the porous polymer matrix after coating.[18] The nanocellulose utilized in membrane applications mostly has wood origins rather than non-wood.[18,19] Nonetheless, nanocellulose extraction from natural non-wood waste/residual material has been considered more efficient in delignification processes due to the lignin content being lower in non-wood than in woody plants.[20]

The utilization of nanocellulose from non-wood materials, for instance oil palm empty fruit bunches (OPEFB), as an additive in membrane composites for bioenergy applications is still unknown. Therefore, in this study, membranes consisting of TOCNs from OPEFB and alginate were investigated in a pervaporation system for water-ethanol mixture separation. Pervaporation is a method for the separation of mixtures of liquids by partial vaporization through a non-porous membrane. The separation mechanism is a solution–diffusion model.[21] The method is particularly useful to separate liquid mixtures with close boiling points, as well as azeotropic mixtures of water and ethanol, on the basis of liquid polarity and interaction with polymer membranes.[22] Among pervaporation membranes reported for water-ethanol separation, alginate-based membranes have gained much attention. This is due to their good membrane forming properties, such as high affinity for water molecules, non-toxicity, low cost, and ease to use, although these membranes also have lower mechanical strength.[23] Therefore, the utilization of nanocellulose in alginate-based membranes is suggested to overcome this disadvantage. Nanocellulose films were prepared by a TEMPO-mediated oxidation (TOCN) process, with a high aspect ratio and mechanical property (tensile strength > 200 MPa).[24] The presence of anionic carboxylate groups on the surface of TOCNs is responsible for improving the hydrophilic properties of the membranes. The presence of water increases membrane permeability and plasticity. Competitive sorption of other gas species may occur, which is important in the case of membrane transport facilitation.[17,25,26] However, studies of pervaporation membranes using alginate- and OPEFB-derived TOCNs have not been reported yet. On the other hand, the use of other polysaccharides, such as chitosan, for alcohol dehydration has been reported intensively.[23,27–29] Nanofibers from OPEFB in membrane applications pave the way for the utilization of low-cost agricultural residues as value-added useful products.

EXPERIMENTAL

Materials

Bleached kraft pulp of oil palm empty fruit bunches (OPEFB) was kindly supplied from Biomaterial Research Institute, Indonesian Institute of Sciences (Bogor, Indonesia). 2,2,6,6-Tetramethylpiperidine 1-oxyl (TEMPO), sodium bromide, sodium hypochlorite and sodium borohydride were purchased from Sigma-Aldrich (Tokyo, Japan) and used without further purification. Sodium alginate (500 cps) was purchased from Nacalai Tesque (Kyoto, Japan). Calcium chloride ($CaCl_2$) was purchased from Wako Pure Chemical (Osaka, Japan). The water used in this study was purified with the Arium Ultrapure Water System (Sartorius Co., Ltd., Tokyo, Japan). The filter holder set up for the pervaporation system was purchased from Toyo Roshi Kaisha Ltd. (Tokyo, Japan), with a filter diameter of 47 mm. The commercial membrane PTFE Advantec Membrane Filter (Toyo Roshi Kaisha, Tokyo, Japan), of 0.5 µm pore size, was used for comparison, denoted as PTFE membrane. Ethanol (99.5%) was purchased from Fujifilm Wako Pure Chemical, Osaka, Japan, and used without further purification.

Methods

Preparation and characterization of OPEFB-derived TOCNs

The preparation of TOCNs from OPEFB was performed as described in our previous study, using 20 mmol of oxidant (NaClO) by TEMPO-mediated oxidation.[30] The resultant TOCN from OPEFB was denoted as op-TOCN. Meanwhile, wood-based TOCN from Nippon Paper Company was used for comparison and denoted as w-TOCN. Carboxylate contents were measured by conductometric titration.[31] The carboxylate content of OPEFB-derived TOCN was 1.50 mmol/g, and that of wood-derived TOCN was 1.59 mmol/g.

The morphology of TOCNs was observed on a Transmission Electron Microscope (TEM), JEM-2100 HC (JEOL Ltd., Tokyo, Japan), operated at an accelerating voltage of 120 kV, at the Ultramicroscopy Research Center of Kyushu University. The crystallinity index of TOCNs was recorded on a Rigaku X-ray-Diffractometer/XRD (Rigaku Denki Co. Ltd., Tokyo, Japan) operated at 40 kV and 20 mA. Details of the procedure for observing the morphology of TOCNs using TEM and the crystallinity index of TOCNs using XRD have been provided in our previous study.[11]

Preparation of TOCN-alginate membranes cross-linked with $CaCl_2$

About 300 mg of sodium alginate was dissolved in 30 mL of deionized water (DI) by vigorous stirring at room temperature until complete dissolution. Twenty-five mL of 0.4 wt% op-TOCN suspension (100 mg of dry weight) was added, and the mixture was stirred for 2 h and poured into a PTFE Petri dish. Membranes were dried at room temperature for 2-3 days. The dried membranes were then peeled off carefully. The obtained membranes were cross-linked with $CaCl_2$ by immersion in 5% (v/v) calcium chloride ($CaCl_2$) for 3 h, rinsed with DI water and dried in ambient air for 2 days. The obtained membrane composed of alginate and op-TOCN was then denoted as op-TOCN-A. The same preparation was applied to the membrane from alginate with commercially available TOCN (w-TOCN), denoted as w-TOCN-A. A membrane made of alginate without TOCNs (alginate w/o TOCN) was prepared as control. A commercial hydrophobic PTFE membrane (Advantec Membrane Filter, Toyo Roshi Kaisha Ltd., Tokyo, Japan) was used for comparison. The experimental scheme of the research is illustrated in Figure 1.

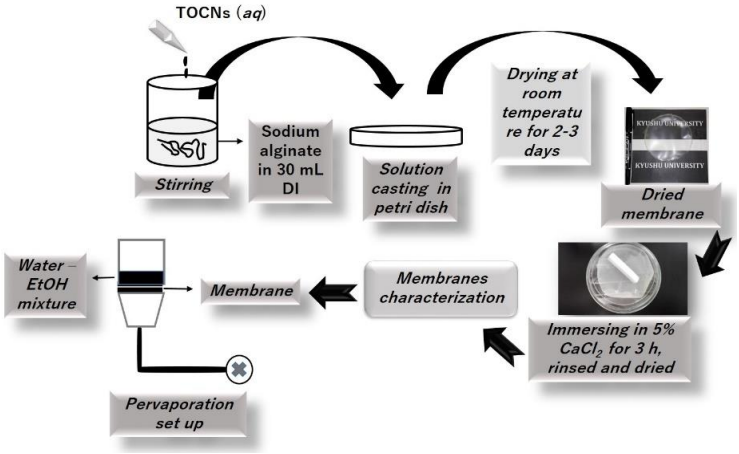

Figure 1: Experimental scheme of the preparation of alginate-TOCN membranes and their use for water-ethanol separation

Membrane characterization

Membrane characterization included microscopic observation and observation of membrane thickness and water content. Microscopic observation was performed by taking cross-sectional and surface images by Scanning Electron Microscopy (Zeiss ULTRA 55, USA) at the Ultramicroscopy Research Center, Kyushu University, Japan. The observation was conducted at an acceleration voltage of 5 kV. Thin gold layers were coated on the surfaces of the samples before observation using a JEOL JFC-1600 Autofine Coater (Japan Electronic Corporation Ltd., Tokyo, Japan) at 30 mA for 10 s. Membrane thickness was measured using a Digital Micrometer (Series 406-Non Rotating Spindle Type 406-250, Mitutoyo Corp., Kawasaki, Japan).

Water contents were calculated using the following equation:

$$\text{Water content (\%)} = (W_{initial} - W_{dry}) / W_{inital} \times 100 \qquad (1)$$

where $W_{initial}$ is the weight of membrane in the initial condition (before drying) and W_{dry} is the weight of dried membrane after exposure to a temperature of 103 °C for 1 h. All membranes were kept on a desiccator after cooling and then weighed.

Fourier Transform Infrared (FTIR) analysis was conducted using an FTIR spectrometer (JASCO FT/IR-680 TypeA, Japan) at the Center of Advanced Instrumental Analysis, Kyushu University, Japan. The analysis was

conducted in the spectral range of 400-4000 cm^{-1}.

The contact angles of resultant membranes were observed using a Drop Master 300 K. Samples were made by cutting the membranes into sheets approximately 10 mm x 50 mm in size. The contact angles were measured at four different spots by dropping a droplet (1 µL) of DI water on each membrane sample and averaging the values obtained.

The absorption capacity of membranes in water and absolute ethanol was determined by immersing dried membranes (dry weight W_d) in an appropriate liquid until a condition of equilibrium was reached. The liquid-hydrated membranes were weighed (W_w), and the absorption capacity was calculated using Equation 2:

$$Adsorption\ capacity\ (\%) = \frac{Ww - Wd}{Wd} x\ 100 \quad (2)$$

The surface area and average pore sizes were measured using the Brunauer-Emmett-Teller (BET) method in nitrogen atmosphere. Each sample was dewatered and degassed at 105 °C for 4 h before BET analysis.

Tensile tests of the obtained membranes were performed using Material Testing Instruments (STA-1225, ORIENTEC Co., Ltd., Tokyo, Japan), equipped with a 100 N load cell. The membrane samples were cut into sheets 40-50 mm x 0.7-10 mm in size. Measurement was carried out at 20 mm of active length at 10% min^{-1}.[32]

Pervaporation experiment

The pervaporation set-up schematically shown in Figure 2 consisted of a feed glass tube, a membrane filter holder, a cold trap for permeate and a vacuum pump. Due to difficulties to control the desired pressure, the pressure during the experiment was recorded, ranging from 30 to 40 hPa. The feed across the membrane and the permeate were collected in the cold trap, and the collecting time was recorded. The water content was measured using the hybrid titration method by Karl Fischer Moisture Titrator Kyoto-Chem MKH-700 (Kyoto Denshi Kogyo, Kyoto, Japan). The flux (J) and selectivity (α) were calculated using the equation of mass-time data below:

$$J = \frac{Q}{At} \quad (3)$$

Because the obtained membranes were not uniform in thickness, the obtained flux values were then normalized using the following equation:

$$Normalized\ flux = J \text{ x (membrane thickness/50 µm)} \quad (4)$$

Meanwhile, the selectivity of the membrane was calculated using the following equation:

$$\alpha = \left(\frac{Wp}{Ep}\right)/\left(\frac{Wf}{Ef}\right) \quad (5)$$

where Q is the mass of permeate collected in the cold trap in time t, A is the effective membrane surface area, α is the sorption selectivity, W_p and E_p are the weight fractions of water and ethanol, respectively, in the permeate, and W_f and E_f are weight fractions of water and ethanol, respectively, in the feed. Pervaporation was applied to a membrane area of 19.625 cm^2.

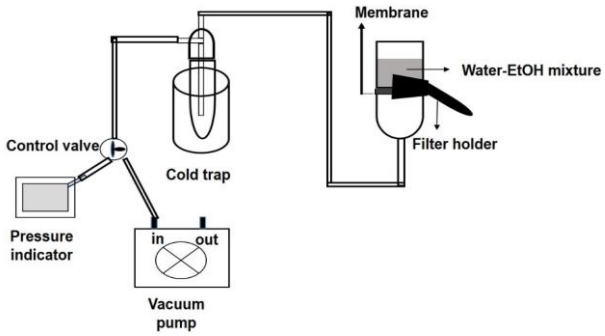

Figure 2: Membrane test scheme

RESULTS AND DISCUSSION

Characterization of TOCNs

The morphologies of OPEFB-derived TOCNs (op-TOCNs) and wood-derived TOCNs (w-TOCNs) are shown in Figure 3A-B. The aspect ratios of op-TOCNs and w-TOCNs were 41±14 and 24±7, respectively. The aspect ratio of OPEFB-derived TOCNs is higher than that of commercial wood-derived TOCNs. This can occur due to differences in the characteristics of wood and non-wood fibers. Besides the fiber characteristics of the original raw material, the pretreatment of cellulose fibers has a major influence on the size of the resulting nanocellulose, although it is not always necessary in the preparation of nanocellulose.[33]

X-ray diffraction (XRD) patterns of op-TOCNs and w-TOCNs are presented in Figure 4. XRD analysis reveals that wood-derived TOCNs (w-TOCNs) have a higher crystallinity index than OPEFB-derived TOCNs (op-TOCNs). The crystallinity index (*Cr.I.*) of w-TOCNs and op-TOCNs was 55% and 60%, respectively. The lower levels of *Cr.I.* of op-TOCNs are not notable. It can be assumed that almost all carboxyl groups formed by the oxidation are present on the surfaces of crystalline cellulose microfibrils.[9] The peaks located at 15º, 22º and 35º are associated to the planes of (110), (200) and (004), respectively.[33] These patterns indicate the characteristics of crystalline cellulose I.[33,34] In addition, the maximum contents of C6-oxidized groups that were formed varied depending on the cellulose I crystal widths. [35]

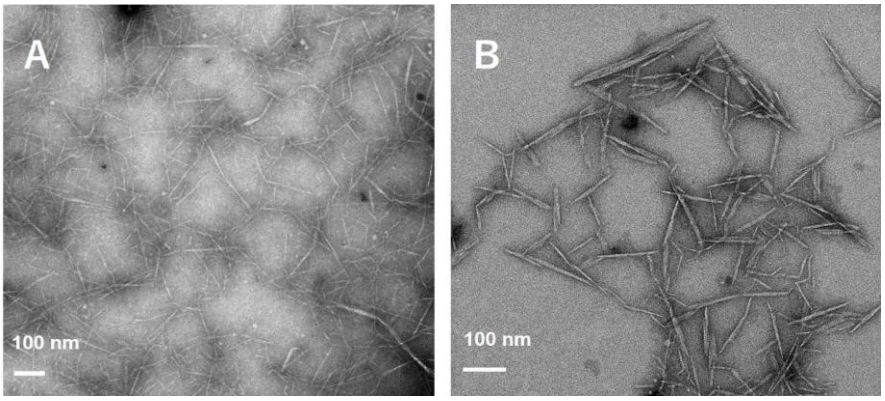

Figure 3: TEM images of (A) op-TOCNs and (B) w-TOCNs

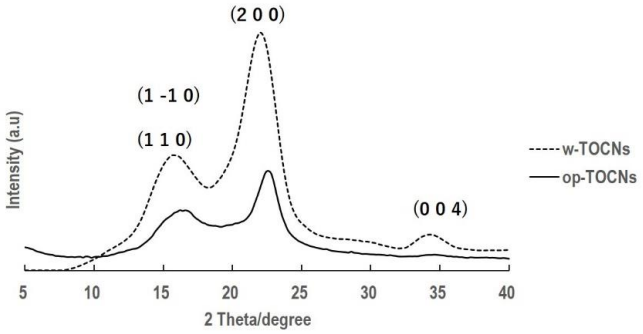

Figure 4: X-ray diffraction patterns of OPEFB-derived TOCNs (op-TOCNs) and wood-derived TOCNs (w-TOCNs)

Membrane morphology

The morphology of the obtained membranes was observed using a Scanning Electron Microscope (SEM) in the surface and cross-sectional areas. Complete images from the SEM analysis are shown in Figure 5. The presence of TOCNs in the alginate-TOCN membranes was confirmed by a fibrous layer appearance in the cross-sectional images (Fig. 5 B-C). This appearance was absent on the control membrane (alginate w/o TOCN). The results revealed by the SEM images are in good agreement with those of a previous reported study.[16] In addition, the surface morphology of the alginate membrane in the presence of TOCNs showed a rougher surface, compared to the control membrane.

The membrane thickness of alginate w/o TOCN, op-TOCN-A, and w-TOCN-A was 52 µm, 82 µm, and 78 µm, respectively. In addition, the water content of alginate w/o TOCN, op-TOCN-A and w-TOCN-A was 6.2%, 5.8% and 3.6%, respectively. The densities of the obtained membranes were 0.81 for alginate w/o TOCN, 0.96 for op-TOCN-A, and 0.73 for w-TOCN-A.

Fourier transform infrared (FTIR) analysis

The FTIR spectra are presented in Figure 6. The spectra of op-TOCN show important absorption bands at 1720 cm^{-1} and 1600 cm^{-1}, which corresponded to functional carboxylate groups –COOH and –COONa, respectively.[36] The spectra of op-TOCN-A at ~1602 cm^{-1} were sharper than those of op-TOCN. A similar appearance was also found in the case of w-TOCN-A spectra. From these peaks, it

was assumed that cross-linking of alginate and $CaCl_2$ had occurred; they exclusively had the carboxylate structures of $(TOCN\text{-}COO)_2Ca$.[37] In the absence of TOCNs, the band at 1600 cm^{-1} of alginate w/o TOCN was broader.

Membrane morphology before and after pervaporation tests

The surface morphology after pervaporation was observed to check whether micro-cracks occurred during the experiment (Fig. 7 D–F). Interestingly, micro-cracks were not observed in the case of op-TOCN-A and w-TOCN-A. Rougher surface appeared after the treatment due to the vacuum pressure applied during the pervaporation set-up. However, op-TOCN-A showed lower surface roughness, compared with w-TOCN-A and alginate w/o TOCN. The optical images of the membranes after the treatment reveal that morphological changes could be detected more distinctly on w-TOCN-A than on op-TOCN-A. It is assumed that a rearrangement of polymer chains in the case of w-TOCN-A might have occurred more intensively than in the case of op-TOCN-A, due to the vacuum pressure applied during the pervaporation process.

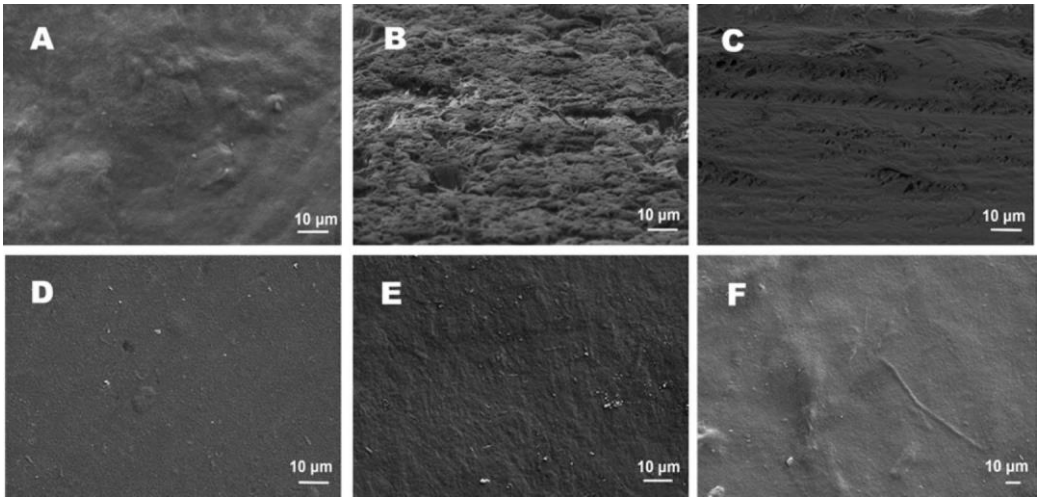

Figure 5: SEM images of cross-sectional (upper) and surface morphology (bottom) of (A, D) alginate w/o TOCN, (B, E) op-TOCN-A, and (C, F) w-TOCN-A (scale bars: 10 µm)

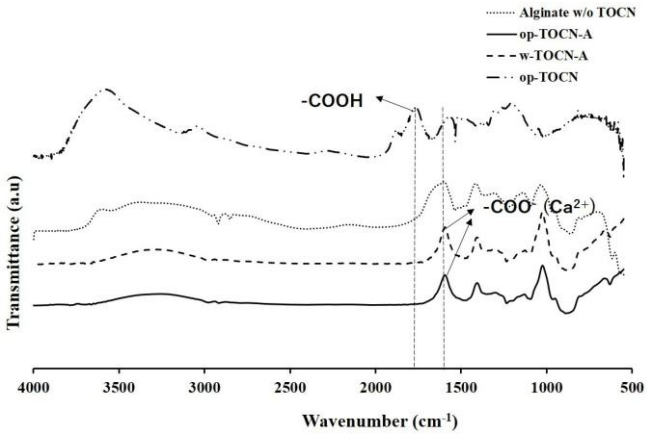

Figure 6: FTIR spectra of TOCN-alginate membranes and original TOCNs from OPEFB

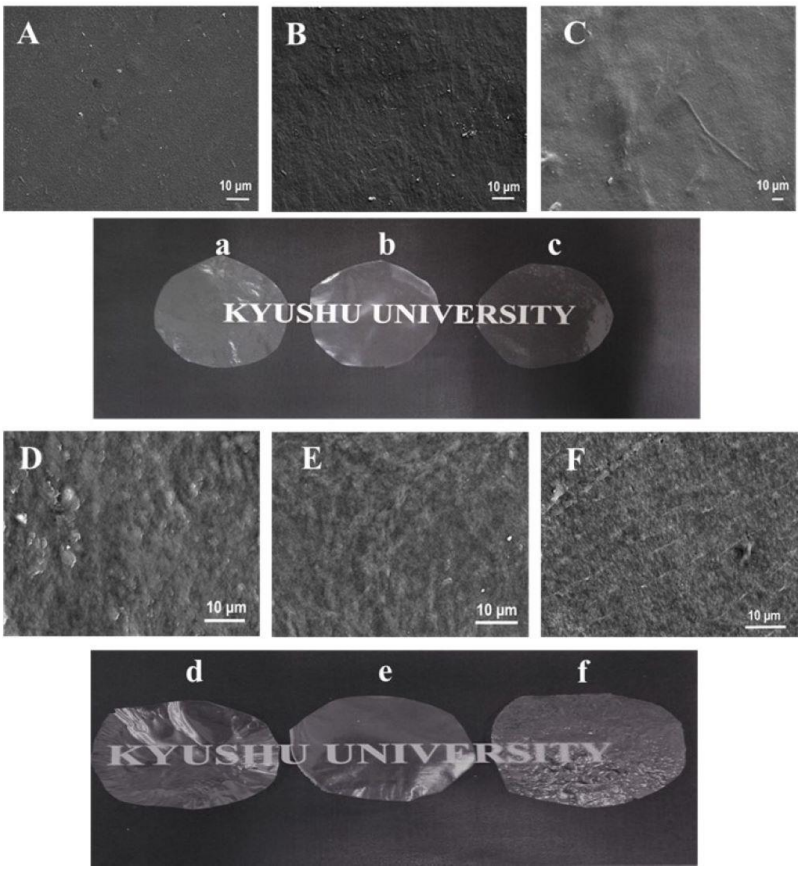

Figure 7: SEM images of membrane surfaces before (A: alginate w/o TOCN; B: op-TOCN-A; C: w-TOCN-A) and after the treatment (D: alginate w/o TOCN; E: op-TOCN-A; C: w-TOCN-A) and optical images of their representatives in lowercase letters (scale bars: 10 μm)

Contact angles

Contact angle measurement was performed using water and water-ethanol mixtures. Actually, measuring a contact angle using absolute ethanol on the surface of membrane was difficult because the ethanol would spread immediately on the membrane surface after dropping. Therefore, the contact angle measurement was conducted on mixtures of water and ethanol (80% water and 20% ethanol and 60% water and 40% ethanol), as shown in Figure 8.

A contact angle is an angle at the interface where water, air and solid meet, and its value is a measure of how likely the surface is to be wetted by water. Low contact angle values demonstrate a tendency of water to spread and adhere to the surface, whereas high contact angle values show the surface's tendency to repel water.[38] The higher the ethanol concentration the lower the contact angle. It is because the surface tension of ethanol, which determines contact angles, is smaller than that of water. The surface tension of an aqueous solution will decrease with an increase in the alcohol concentration.[39] The contact angles of the PTFE membrane were difficult to capture for both water and water-ethanol mixtures. The contact angle of a liquid on a solid surface is a key parameter reflecting wettability. Based on the data in Figure 8, the wettability of the alginate membrane hardly changed in the presence of TOCNs.

Flux, selectivity and surface analysis

A flux analysis was conducted on feeds containing 80% ethanol and 20% water (*v/v*), denoted as 80E20W, and 90% ethanol and 10% water (*v/v*), denoted as 90E10W. The results are as described in Figure 9.

Figure 9 shows that the addition of TOCNs to alginate membranes increased the flux capacity. The cross-linking of TOCNs, alginate and Ca^{2+} ions increased the surface area, induced pore formation and affected the flux. The surface area of the alginate membrane became larger in the presence of w-TOCN in w-TOCN-A (Table 1), resulting a higher flux compared to op-TOCN-A and alginate w/o TOCN. During the pervaporation, the first constructive step in transporting permeating components

through the membrane is sorption of the permeating components from the feed liquid into the membrane. Therefore, larger surface areas are preferable to get higher contact or sorption of permeating components on the membrane surface.[40]

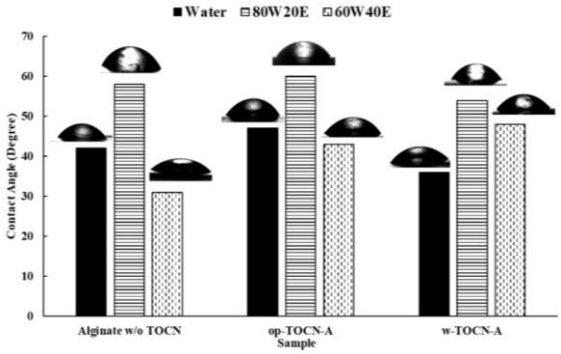

Figure 8: Contact angle measurement for water and water–ethanol mixtures

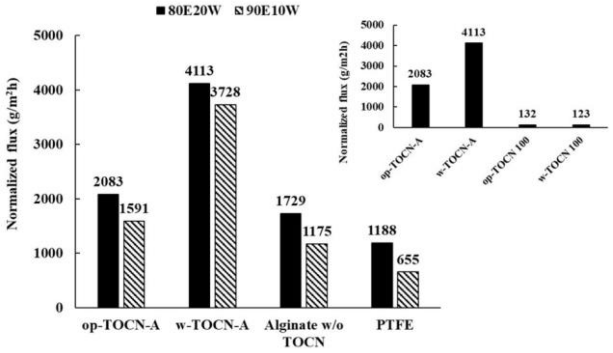

Figure 9: Normalized flux values of alginate, alginate-TOCN and PTFE membranes for water-ethanol mixtures

Table 1
Adsorption capacity, water selectivity and surface analysis

Sample	Adsorption capacity (%)		Water content in permeate (%)[a]		Selectivity[b]		Surface area, $a_{s\ BET}$ (m^2g^{-1})[c]	Ave-rage pore size (nm)[c]
	Water	EtOH	80E20W[b]	90E10W[b]	80E20W	90E10W		
op-TOCN-A	87	8	23.8	11.7	53	56	0.73	37
w-TOCN-A	78	8	17.5	13.1	60	54	1.18	23
Alginate w/o TOCN	66	35	23.8	15.3	45	40	0.90	30
PTFE	32	47	24.3	14.9	42	42	4.69	5000[d]

Note: [a] initial water content in 80E20W was 25.5%, and in 90E10W – 15.62%, measured by a Karl Fischer titrator; [b] selectivity corresponded to water; the collecting time was adjusted to 1 h; [c] based on BET surface analysis with the weight of the measured sample being ~0.1 g; [d] determined by the company/supplier

In addition, op-TOCN-A and alginate w/o TOCN had lower surface areas, but larger pore sizes compared to w-TOCN-A (Table 1). Pore size plays an important role during the second constructive step of pervaporation, which is diffusion of permeating components through the membrane, and the third, which is desorption of permeating components downstream the membrane. Therefore, the flux of op-TOCN-A was slightly higher compared to that of the control membrane (alginate w/o TOCN), because the larger pore size of op-TOCN-A increased the diffusion and desorption rates, while the surface areas of the two membranes were not too different (Table 1). However, according to the mass transfer analysis conducted by Phattaranawik and co-authors, the influence of pore size is insignificant.[41] Alginate and alginate-TOCN membranes have mesopore sizes of 2–50 nm according to IUPAC pore size classification, while PTFE membranes are classified to have macropore sizes of >50 nm.[42]

A comparison with the positive control membranes (op-TOCN100 and w-TOCN100) was conducted at the feed with 80% ethanol and 20% water (inserted picture in Fig. 9). The results revealed that the self-standing TOCN membranes (op-TOCN and w-TOCN) had very low and distinct flux capacities. It is assumed that self-standing TOCN films are not effective as pervaporation membranes. Nanocellulose prepared by TEMPO-mediated oxidation is hydrophilic. Self-standing TOCN films have been reported to have high water vapor permeability of approximately 70 g μm m^{-2} day^{-1} kPa^{-1} at 30% RH.[24] This property needs to be combined with other hydrophilic polymers, such as alginate, for use in pervaporation membranes. Sodium alginate membranes have been acknowledged to have high water solubility and sorption selectivity.[43] Hydrophilic groups absorb water molecules preferentially, which leads to both high flux and high separation factors. However, the introduction of hydrophilic groups sometimes swells the membrane significantly due to its plasticization action, which results in low selectivity.[23]

Furthermore, with the increase in the mass percentage of water in the feed, the membrane swelling

will also increase, and this will create more free volume, which results in an increase in the permeate flux.[44] The flux capacity is affected not only by the mass of water transferred from the feed, but also by the shrinkage of internal pores of the membrane, resulting in flow viscosity and thus total permeation flux.[45]

The hydrophobic membrane, PTFE, showed the largest surface area and the largest pore size, as determined by the supplier. However, the hydrophobic properties of the PTFE membrane lowered the water affinity of this membrane to a great degree, resulting in low water adsorption and flux. The large pore size made the diffusion rate excessively high and caused the water sorption and selectivity to be low.

Tensile tests

The mechanical properties of the obtained membranes are as described in Figure 10. The self-standing alginate membrane (alginate w/o TOCN) showed the lowest mechanical properties. Yang and co-authors reported that alginate membranes cross-linked with cellulose and Ca^{2+} had high mechanical properties. The presence of cellulose and Ca^{2+} caused the membranes to have tensile strength, of up to 47 MPa, and elongation at break of 23%, while the absence of cellulose and Ca^{2+} caused the membranes to have low tensile strength, of only about 4.2 MPa, and elongation at break of 17%.[46] This study revealed that in the presence of TOCNs, in the case of both op-TOCN and w-TOCN, the tensile strength and elongation at break of alginate membranes improved twice and by 5 times, respectively. The higher improvement found in w-TOCN than that in op-TOCN might be caused by the differences in the cellulose contents of woody and non-woody nanocellulose starting materials. Moreover, the higher crystallinity index in w-TOCN corresponds to increases in rigidity of the cellulose structure and leads to higher tensile properties.[47] However, this result emphasized the potential utilization of low-cost agricultural residues as an enhancer in membrane composites.

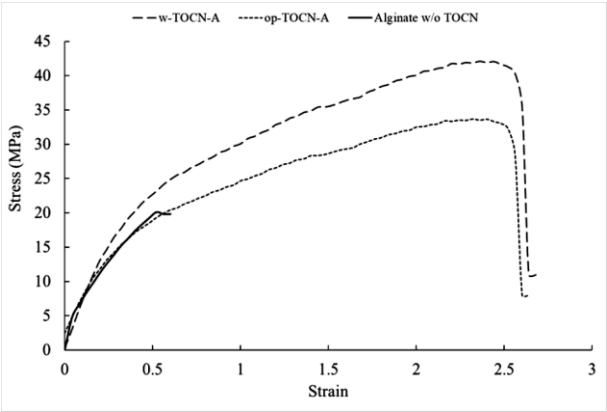

Figure 10: Tensile strength of alginate and alginate-TOCN membranes

CONCLUSION

The utilization of OPEFB-derived nanocellulose, prepared by TEMPO-mediated oxidation in pervaporation membranes (op-TOCN-A) revealed that the addition of OPEFB-derived nanocellulose to an alginate matrix, followed by cross-linking with Ca^{2+}, induced pore formation and slightly increased the flux capacity. However, its performance was lower but still comparable to the performance of woody TOCNs in alginate matrix (w-TOCN-A) with respect to flux capacity, water selectivity and mechanical properties. The addition of hydrophilic materials, such as TOCNs, to alginate improved the flux capacity, water sorption and selectivity in pervaporation membranes. Furthermore, membrane engineering (including membrane composition and preparation) and pervaporation conditions (the pressure applied, temperature and feed flow rate) might determine the membrane performance. Therefore, a further study into the utilization of nanocellulose in pervaporation membranes is needed to figure out the optimum conditions of nanocellulose application in membrane composites for achieving optimum membrane permeability and selectivity.

ACKNOWLEDGEMENTS: This research was supported by the Advanced Low Carbon Technology Research and Development Program of the Japan Science and Technology Agency (T.K.) and the

Research Fellowship for Young Scientists of the Japan Society for the Promotion of Science (K.K.). The authors are grateful to Hendrik Setiawan from the Department of Hydrogen Energy Systems, Faculty of Engineering, Kyushu University for kindly providing assistance in the surface analysis. Thanks are also due to the Ministry of Education and Culture of the Republic of Indonesia for the partial financial support through the Beasiswa Unggulan Program.

REFERENCES

[1] BPS-Statistics Indonesia, *Indonesian Oil Palm Statistics* (BPS-Statistics Indonesia, 2018), https://www.bps.go.id/.../statistik-kelapa-sawit-indonesia-2018.html
[2] Directorat General of Estate Crops, *Tree Crop Estate Statistics of Indonesia 2014-2016* (2015), http://ditjenbun.pertanian.go.id/tinymcpuk/gambar/file/statistik/2016/SAWIT 2014-2016.pdf
[3] M. S. Umikalsom, A. B. Ariff, H. S. Zulkifli, C. C. Tong, M. A. Hassan *et al*., *Bioresour. Technol*., **62**, 1 (1997), https://doi.org/10.1016/S0960-8524(97)00132-6
[4] K. Myrtha, H. Onggo, A. H. Dawam Abdullah and A. Syampurwadi, *J. Biol. Sci*., **8**, 101 (2008), https://doi.org/10.3923/jbs.2008.101.106
[5] Z. A. Zianor Azrina, M. D. H. Beg, M. Y. Rosli, R. Ramli, N. Jonadi *et al*., *Carbohyd. Polym*., **162**, 115 (2017), https://doi.org/10.1016/j.carbpol.2017.01.035
[6] T. Abitbol, A. Rivkin, Y. Nevo, E. Abraham, T. Ben-Shalom *et al*., *Curr. Opin. Biotechnol*., **39**, 76 (2016), https://doi.org/10.1016/j.copbio.2016.01.002
[7] P. Bajpai, "Pulp and Paper Industry Nanotechnology in Forest Industry", Elsevier Inc., 2016, pp. 27-40
[8] T. Isogai, T. Saito and A. Isogai, *Biomacromolecules*, **11**, 1593 (2010), https://doi.org/10.1021/bm1002575
[9] R. Tanaka, T. Saito and A. Isogai, *Int. J. Biol. Macromol*., **51**, 228 (2012), https://doi.org/10.1016/j.ijbiomac.2012.05.016
[10] A. Isogai, T. Saito and H. Fukuzumi, *Nanoscale*, **3**, 71 (2011), https://doi.org/10.1039/c0nr00583e
[11] N. Hastuti, K. Kanomata and T. Kitaoka, *J. Polym. Environ*., **26**, 3698 (2018), https://doi.org/10.1007/s10924-018-128-x
[12] D. Cheng, Y. Wen, X. An, X. Zhu and Y. Ni, *Carbohyd. Polym*., **151**, 326 (2016), https://doi.org/10.1016/j.carbpol.2016.05.083
[13] R. Endo, T. Saito and A. Isogai, *Polymer* (*United Kingdom*), **54**, 935 (2013), https://doi.org/10.1016/j.polymer.2012.12.035
[14] N. Zhang, G. L. Zang, C. Shi, H. Q. Yu and G. P. Sheng, *J. Hazard. Mater*., **316**, 11 (2016), https://doi.org/10.1016/j.jhazmat.2016.05.018
[15] D. Celebi, R. H. Guy, K. J. Edler and J. L. Scott, *Int. J. Pharm*., **514**, 238 (2016), https://doi.org/10.1016/j.ijpharm.2016.09.028
[16] T. Suratago, S. Taokaew, N. Kanjanamosit, K. Kanjanaprapakul, V. Burapatana *et al*., *J. Ind. Eng. Chem*., **32**, 305 (2015), https://doi.org/10.1016/j.jiec.2015.09.004
[17] L. Ansaloni, J. Salas-Gay, S. Ligi and M. G. Baschetti, *J. Membr. Sci*., **522**, 216 (2017), https://doi.org/10.1016/j.memsci.2016.09.024
[18] P. Hadi, M. Yang, H. Ma, X. Huang, H. Walker *et al*., *J. Membr. Sci*., **579**, 162 (2019), https://doi.org/10.1016/j.memsci.2019.02.059
[19] J. Ø. Torstensen, R. M. L. Helberg, L. Deng, Ø. W. Gregersen and K. Syverud, *Int. J. Greenh. Gas Control*., **81**, 93 (2019), https://doi.org/10.1016/j.ijggc.2018.10.007
[20] O. Nechyporchuk, M. N. Belgacem and J. Bras, *Ind. Crop. Prod*., **93**, 2 (2016), https://doi.org/10.1016/j.indcrop.2016.02.016
[21] P. Wei, H. Cheng, L. Zhang, X. H. Xu, H. L. Chen *et al*., *Renew. Sustain. Energ. Rev*., **30**, 388 (2014), https://doi.org/10.1016/j.rser.2013.10.017
[22] U. S. Toti and T. M. Aminabhavi, *J. Appl. Polym. Sci*., **85**, 2014 (2002), https://doi.org/10.1002/app.10816
[23] G. Y. Moon, R. Pal and R. Y. M. Huang, *J. Membr. Sci*., **156**, 17 (1999), https://doi.org/10.1016/S0376-7388(98)00322-6
[24] H. Fukuzumi, T. Saito and A. Isogai, *Carbohyd. Polym*., **93**, 172 (2013), https://doi.org/10.1016/j.carbpol.2012.04.069
[25] M. G. Baschetti, M. Minelli, J. Catalano and G. C. Sarti, *Int. J. Hydrogen Energ*., **38**, 11973 (2013), https://doi.org/10.1016/j.ijhydene.2013.06.104
[26] G. Q. Chen, C. A. Scholes, G. G. Qiao and S. E. Kentish, *J. Membr. Sci*., **379**, 479 (2011), https://doi.org/10.1016/j.memsci.2011.06.023
[27] Y. J. Han, K. H. Wang, J. Y. Lai and Y. L. Liu, *J. Membr. Sci*., **463**, 17 (2014), https://doi.org/10.1016/j.memsci.2014.03.052
[28] M. Ghazali, M. Nawawi and R. Y. M. Huang, *J. Membr. Sci*., **124**, 53 (1997), https://doi.org/10.1016/S0376-7388(96)00216-5
[29] T. Uragami, T. Saito and T. Miyata, *Carbohyd. Polym*., **120**, 1 (2015),

https://doi.org/10.1016/j.carbpol.2014.11.032
[30] N. Hastuti, K. Kanomata and T. Kitaoka, in *Procs. International Conference on Forest Products IOP Conference Series: Earth and Environmental Science*, Bogor, 2 November, 2019, Vol. 359, pp. 1-7
[31] T. Saito and A. Isogai, *Biomacromolecules*, **5**, 1983 (2004), https://doi.org/10.1021/bm0497769
[32] K. Tsuboi, S. Yokota and T. Kondo, *Nord. Pulp Pap. Res. J.*, **29**, 69 (2014), https://doi.org/10.3183/npprj
[33] X. Miao, J. Lin, F. Tian, X. Li, F. Bian *et al.*, *Carbohyd. Polym.*, **136**, 841 (2016), https://doi.org/10.1016/j.carbpol.2015.09.056
[34] J. Chandra, N. George and S. K. Narayanankutty, *Carbohyd. Polym.*, **142**, 158 (2016), https://doi.org/10.1016/j.carbpol.2016.01.015
[35] A. Isogai, T. Saito and H. Fukuzumi, *Nanoscale*, **3**, 71 (2011), https://doi.org/10.1039/C0NR00583E
[36] S. Fujisawa, Y. Okita, H. Fukuzumi, T. Saito and A. Isogai, *Carbohyd. Polym.*, **84**, 579 (2011), https://doi.org/10.1016/j.carbpol.2010.12.029
[37] M. Shimizu, T. Saito and A. Isogai, *J. Membr. Sci.*, **500**, 1 (2016), https://doi.org/10.1016/j.memsci.2015.11.002
[38] T. Huhtamäki, X. Tian, J. T. Korhonen and R. H. A. Ras, *Nat. Protoc.*, **13**, 1521 (2018), https://doi.org/10.1038/s41596-018-0003-z
[39] L. T. Fan, X. G. Yuan, C.-X. Zhou, A. W. Zheng, K. T. Yu *et al.*, *Chem. Eng. Technol.*, **34**, 1535 (2011), https://doi.org/10.1002/ceat.201000474
[40] Y. K. Ong, G. M. Shi, N. L. Le, Y. P. Tang, J. Zuo *et al.*, *Prog. Polym. Sci.*, **57**, 1 (2016), https://doi.org/10.1016/j.progpolymsci.2016.02.003
[41] J. Phattaranawik, R. Jiraratananon and A. G. Fane, *J. Membr. Sci.*, **215**, 75 (2003), https://doi.org/10.1016/S0376-7388(02)00603-8
[42] B. D. Zdravkov, J. J. Čermák, M. Šefara and J. Janků, *Cent. Eur. J. Chem.*, **5**, 385 (2007), https://doi.org/10.2478/s11532-007-0017-9
[43] C. K. Yeom, J. G. Jegal and K. H. Lee, *J. Appl. Polym. Sci.*, **62**, 1561 (1996), https://doi.org/10.1002/(SICI)1097-4628(19961205)62:10<1561::AID-APP8>3.0.CO;2-M
[44] M. D. Kurkuri and T. M. Aminabhavi, *J. Appl. Polym. Sci.*, **89**, 300 (2003), https://doi.org/10.1002/app.12087
[45] X. Shu, X. Wang, Q. Kong, X. Gu and N. Xu, *Ind. Eng. Chem. Res.*, **51**, 12073 (2012), https://doi.org/10.1021/ie301087u
[46] G. Yang, L. Zhang, T. Peng and W. Zhong, *J. Membr. Sci.*, **175**, 53 (2000), https://doi.org/10.1016/S0376-7388(00)00407-5
[47] M. K. M. Haafiz, S. J. Eichhorn, A. Hassan and M. Jawaid, *Carbohyd. Polym.*, **93**, 628 (2013), https://doi.org/10.1016/j.carbpol.2013.01.035